Fiber coating with surfactant solutions

Amy Q. Shen and Blake Gleason
Division of Engineering & Applied Sciences, Harvard University, Cambridge, Massachusetts 02138

Gareth H. McKinley
Hatsopoulos Microfluids Laboratory, Department of Mechanical Engineering, Massachusetts Institute of Technology, Cambridge, Massachusetts 02139

Howard A. Stone
Division of Engineering & Applied Sciences, Harvard University, Cambridge, Massachusetts 02138

(Received 14 November 2001; accepted 15 August 2002; published 7 October 2002)

When a fiber is withdrawn at low speeds from a pure fluid, the variation in the thickness of the entrained film with imposed fiber velocity is well-predicted by the Landau–Levich–Derjaguin (LLD) equation. However, surfactant additives are known to alter this response. We study the film thickening properties of the protein BSA (bovine serum albumin), the nonionic surfactant Triton X-100, and the anionic surfactant SDS (sodium dodecyl sulfate). For each of these additives, the film thickening factor α (the ratio of the measured thickness to the LLD prediction) for a fixed fiber radius varies as a function of the ratio of the surfactant concentration c to the critical micelle concentration (CMC). In the case of BSA, which does not form micelles, the reference value is the concentration at which multilayers form. As a result of Marangoni effects, α reaches a maximum as c approaches the CMC from below. However, when the surfactant concentration c exceeds the CMC, the behavior of α varies as a consequence of the dynamic surface properties, owing for example to different sorption kinetics of these additives, or possibly surface or bulk rheological effects. For SDS, α begins to decrease when c exceeds the CMC and causes the surface to become partially or completely remobilized, which is consistent with the experimental and theoretical results published for studies of slug flows of bubbles and surfactant solutions in a capillary tube and the rise of bubbles in surfactant solutions. However, when the SDS or Triton X-100 surfactant concentration is well above the CMC, we observe that the film thickening parameter α increases once again. In the case of SDS we observe a second maximum in the film thickening factor. For all the experiments, transport of monomers to the interface is limited by diffusion and the second maximum in the film thickening factor may be explained as a result of a nonmonotonic change in the stability characteristics of suspended SDS micelles and corresponding changes in the rheology of the solution. © *2002 American Institute of Physics.* [DOI: 10.1063/1.1512287]

I. INTRODUCTION

Coating flows are ubiquitous in industrial processing. The coating materials protect, functionalize, and lubricate surfaces. Typically the coating is a thin layer of a liquid applied to a solid substrate in a dynamic manner and there is a large literature on different coating configurations and their fluid dynamics.[1] One area that has received less attention is the coating response of complex fluids, such as surfactant solutions.[2,3] In this paper we report the results of our experimental studies of the coating of micron-sized fibers by three different surfactant solutions.

The classic film-coating problem dates back to early work of Landau and Levich[4] and Derjaguin.[5] These authors determined how the coating thickness depends on the substrate speed (U) and geometry (e.g., plate or fiber) in the low capillary number limit, $\mathcal{C}=\mu U/\gamma \ll 1$, where μ is the fluid shear viscosity and γ is the fluid surface tension. We refer to these contributions collectively as LLD. Recent work on this general problem, including extensive experimental verifications, is summarized by Quéré.[3]

Most research has focused on coating with Newtonian fluids.[4–7] However, in practice, many important coating liquids are complex fluids consisting of surfactant solutions, mixed surfactant systems, polymer solutions, or suspensions. Therefore, surface tension variations, the bulk rheology, as well as the surface rheology, of these complex fluids impact the coating properties.

Quéré and his coworkers have conducted several studies of the fiber-coating problem with complex fluids[2,3,8–10] and we build on their work here. They studied fiber coating with one type of surfactant [sodium dodecyl sulphate (SDS)] with bulk concentrations varied between 0.01 and 10.0 times the critical micelle concentration (CMC). They observed that the film tended to thicken when SDS was present in the solution compared to that of a pure solution and they quantified several features of the dynamical response, as discussed further below. Also, de Ryck and Quéré[10] reported coating of semidilute polymer solutions (polyethylene oxide) onto a wire and observed that the film thickened significantly due to the normal stresses produced by the polymer solution; see also Tallmadge[11] who examined the analogous plate-coating

 © 2002 American Institute of Physics

Downloaded 03 Jan 2003 to 18.80.1.86. Redistribution subject to AIP license or copyright, see http://ojps.aip.org/phf/phfcr.jsp

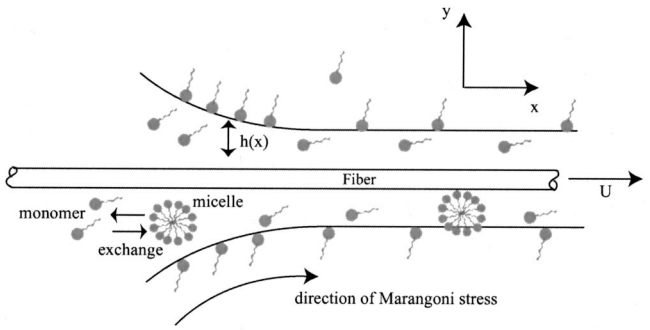

FIG. 1. Sketch of a fiber passing through a fluid bath. The presence of surfactants at the interface and in bulk as monomers and micelles is also indicated.

problem. Finally, Quéré and de Ryck briefly studied fiber coating with emulsions.[12]

In coating problems, the mechanism for the observed film thickening with the surfactant solution is due to stretching of the interface, as it is dragged out from the meniscus, which alters the surface concentration of surfactant and hence the variation of surface tension along the interface (see Fig. 1). Motion induced by this surface tension gradient is usually referred to as a Marangoni effect. For the case of fiber coating with surfactant solutions, Marangoni stresses due to the varying distribution of surfactant additives between the continuous film region and the meniscus can generate an extra traction along the pulling direction *towards* the film and lead to the thickening of the film. It is worth noting that surface tension gradients can also be induced chemically or thermally[13–15] and their role in thin-film flows has many similarities with the fiber-coating problems.

The Marangoni-induced thickening of thin films has been observed in different coating systems. For example, for surfactant concentrations below the CMC, Stebe *et al.*[16] observed an increase in the pressure drop across a bubble in the case of a surfactant-laden slug flow (a train of bubbles and liquid drops in a tube) as compared to the clean fluid case, where the increase of the pressure drop implies a thickening of the thin film between the tube and the bubbles and drops. This configuration is closely related to the study of Bretherton[6] who considered a bubble moving inside a circular tube at low Reynolds and capillary numbers. First, a clean bubble was examined and then the influence of surfactants was treated theoretically by applying a no-slip condition at the interface, thereby assuming a rigid film without accounting for the surfactant transport mechanisms. The theoretical results showed that the film thickness increases (compared to the clean bubble case) by a factor of $2^{2/3}$, which underpredicted Bretherton's experimental results. Ratulowski and Chang[17] showed that the film thickness can be increased by a maximum factor of $4^{2/3}$ if the surfactant transport in the thin film is limited by mass transfer from the bulk phase ahead of the bubble so that Marangoni stresses have a maximal effect (see the Appendix). The same thickening factor of $4^{2/3}$ was derived by Park[18] for dip coating with an insoluble surfactant, i.e., a solid plate pulled at constant velocity vertically out of a fluid bath.

The influence of surfactants does not simply lead to a monotonic thickening of the film with an increase in surfactant concentration. In fact, for concentrations on the order of, and greater than, the CMC, the film thickness can decrease with increasing surfactant concentration. One of the first demonstrations of this fact was made by Stebe *et al.*,[16,19] who observed a decrease of the pressure drop in the slug flow experiment mentioned above, as the surfactant bulk concentration increased above the critical micelle concentration; they interpreted this response as evidence of ''interface remobilization,'' which can be thought of as unretarded surface flow even at high bulk surfactant concentrations. The experimental results are consistent with the idea that micelles present at these high surfactant concentrations act as monomer sources that continually replenish the interface, thus maintaining the interfacial tension at low values everywhere and eliminating surface tension gradients. In fiber-coating studies with SDS, Quéré *et al.*[2] showed that the film thickness on the fiber decreases for surfactant bulk concentrations $c > \mathrm{CMC}$ and they interpreted their results in a manner consistent with the surface remobilization model. Very recently, Ybert and di Meglio[20] performed experiments with rising bubbles in surfactant solutions. They observed results for small molecule surfactants (alcohols dissolved in water) in which Marangoni stresses were often smaller than expected (at least qualitatively) when surfactants are present and again the results were consistent with surface remobilization at high surfactant concentrations.

Despite the present knowledge on coating problems, many important questions regarding coating with surfactant solutions still remain open. For example, little is known about how the film thickness changes as the surfactant concentration is increased much above the critical micelle concentration, how the coating thickness responds to different types of surfactants which have different adsorption and desorption kinetics, or how coating is influenced by multiple surfactant or surfactant–polymer systems. In this article, we provide a series of systematic experimental results describing the coating thickness as a function of the flow dynamics, surfactant concentration, and surfactant kinetic properties. We study the film thickening properties of the protein BSA, the nonionic surfactant Triton X-100, and the anionic surfactant SDS, with particular attention given to high surfactant loadings. We find that surfactants tend to thicken the film as the bulk concentration is increased from zero, which is in agreement with many of the studies mentioned above. However, when the surfactant concentration c exceeds the critical micelle concentration, the film thickness may first decrease, and then may subsequently increase again, which implies that different sorption kinetics of surfactants, and perhaps non-Newtonian rheological responses can alter the local flow dynamics, and hence the film thickness. The qualitative and quantitative details depend on the surfactant system.

A final point to be noted is that in the physical chemistry literature there is experimental evidence that is consistent with the idea that the stability characteristics of surfactant micelles are dependent on the bulk concentration of surfactant, e.g., Patist *et al.*[21] and Huibers.[22] Consequently, in dynamical situations in which interfacial area is created, the

Downloaded 03 Jan 2003 to 18.80.1.86. Redistribution subject to AIP license or copyright, see http://ojps.aip.org/phf/phfcr.jsp

ability of the micelles to act as sources of the monomer is related to the stability of the micelles (i.e., the kinetic rates at which a micelle disintegrates into many monomers or reforms as a micelle). We shall present experimental evidence of fiber coating with the ionic surfactant SDS that is consistent with the idea that there is a range of (high) surfactant concentrations over which micellar stability is increased. Thus, the micelles are less able to act as efficient monomer sources to replenish the newly created surface, and so films become thicker, rather than thinner, with increasing surfactant concentration. Such a response requires that transport is diffusion limited with a time scale comparable to that for micelle disintegration, as described in Sec. VI. This result is one of the main findings of our work.

In Sec. II we provide a brief overview of standard characterizations useful for fiber coating and some basic background on surfactants and micellar stability. The experimental procedure is described in Sec. III. In Sec. IV we cover experimental results while Sec. V provides a discussion and conclusion.

II. BACKGROUND

A. Dimensional analysis and the LLD relation

The study of fiber coating with a Newtonian fluid (without the presence of surfactants) relates the coating thickness h to the fiber radius b, fiber speed U, the interfacial tension γ, fluid viscosity μ, fluid density ρ, and the gravitational acceleration g, so

$$h = f(b, U, \gamma, \mu, \rho, g). \tag{1}$$

Hence, by dimensional analysis, the scaled film thickness h/b can be expressed as

$$\frac{h}{b} = F\left(\frac{\mu U}{\gamma}, \frac{\rho U b}{\mu}, \frac{\rho g b^2}{\gamma}\right), \tag{2}$$

where $\mathcal{C} = \mu U/\gamma$ is the capillary number, $\mathcal{R} = \rho U b/\mu$ is the Reynolds number, and $\mathcal{B} = \rho g b^2/\gamma$ is the Bond number. In our experiments, the fiber radius is $b = 0.038$ mm, the fiber speed is normally varied in the range $0.1 \leqslant U \leqslant 3$ m/s, the fluid viscosities vary between $10^{-3} \leqslant \mu \leqslant 3 \times 10^{-3}$ Pa·s, and the surface tension is in the range of $0.035 \leqslant \gamma \leqslant 0.072$ N/m. For our experiments the Bond number is small and we pull the fiber horizontally so that gravitational effects can be neglected. Further, the influence of inertia is often small. Therefore, we expect

$$\frac{h}{b} = F\left(\frac{\mu U}{\gamma}\right), \tag{3}$$

which expresses the fact that the coating thickness is the result of the competition between viscous forces and flows due to capillarity. Landau and Levich[4] and Derjaguin[5] have analytically derived a law describing this balance for the fiber-coating problem at $\mathcal{C} \ll 1$, and the so-called LLD relation for the fiber coating film thickness is

$$\frac{h}{b} = 1.34\mathcal{C}^{2/3}. \tag{4}$$

In many practical situations, fiber-coating processes are operated in the regime where the coating speed is high and then inertia becomes important; e.g., see Quéré and de Ryck.[8] The LLD relation above has neglected the influence of inertia. Based upon dimensional arguments, Quéré and de Ryck[8] proposed an expression for the coating thickness that introduces the Weber number $\mathcal{W} = \rho U^2 b/\gamma = \mathcal{C}^2 \mathcal{O}_h^{-2}$ in the form

$$\frac{h}{b} = \frac{1.34\mathcal{C}^{2/3}}{1 - \beta\mathcal{W}} = \frac{1.34\mathcal{C}^{2/3}}{1 - \beta\mathcal{C}^2\mathcal{O}_h^{-2}}, \tag{5}$$

where the Ohnesorge number, $\mathcal{O}_h = \mu/(\rho b \gamma)^{1/2}$, is only dependent on material and geometrical parameters and β is a constant which can be determined through curve fitting experimental data (see also Tallmadge and White[7]). This result shows that the film thickness rapidly increases for $\mathcal{C}_{\text{crit}} \approx \mu/(\rho b \gamma)^{1/2}$. In addition, de Ryck and Quéré[23] presented a more detailed model and obtained

$$\frac{h}{b} = \frac{1.34\mathcal{C}^{2/3}}{1 - \beta(h)\mathcal{W} - 1.34\mathcal{C}^{2/3}} = \frac{1.34\mathcal{C}^{2/3}}{1 - \beta(h)\mathcal{C}^2\mathcal{O}_h^{-2} - 1.34\mathcal{C}^{2/3}}, \tag{6}$$

where $\beta(h) = \frac{1}{5}(\ln(R/h) - 3)$, with R the radius of the fluid reservoir; now β varies slowly with changes in film thickness. Equation (6) reduces to (5) when $\mathcal{O}_h \ll 1$. Equations (5) and (6) are consistent with the experimental data (see Figs. 4 and 14 later). The above ideas are useful for organizing results obtained during coating with surfactant solutions, as summarized in Sec. IV.

B. Surfactants

Surfactants typically are amphiphilic molecules with hydrophilic and hydrophobic domains and they are surface active so they can greatly influence the mechanical properties of an interface. Often, surfactants are present simply as contaminants. Through adsorption on interfaces, these molecules generally reduce the surface tension. A surfactant can be categorized based on its polar head groups. Traditionally, there are three types: anionic surfactants, which carry a negative charge, e.g., soap and dishwashing detergents; nonionic surfactants, which have no electrical charge, e.g., laundry detergents and rinse aids; and cationic surfactants, which carry a positive charge, e.g., fabric softeners; for more details see Adamson and Gast.[24] We investigate fiber coating with all three surfactant types.

At high enough surfactant concentrations, the surfactant monomers often form spherical aggregates, or micelles, in the bulk solution. The concentration at which micelle formation begins is called the critical micelle concentration or CMC. The presence of micelles, and their stability, is important for problems in which interfacial area is rapidly created, as in fiber coating. Since the surface concentration of surfactant is reduced by the interfacial stretching accompanying thin-film formation, the primary role of micelles is to act as

Downloaded 03 Jan 2003 to 18.80.1.86. Redistribution subject to AIP license or copyright, see http://ojps.aip.org/phf/phfcr.jsp

sources of surfactant, which thus tend to reduce the surface tension gradient, and so influence the rate at which fluid is delivered to the moving fiber.

In the free-surface flow of a surfactant solution, a surface tension gradient can be induced because the surface concentration of surfactant is nonuniform. Previous research by Carroll and Lucassen[25] and Quéré and coworkers[2,3,8] has shown that the film tends to thicken when a surfactant is present in the solution compared to that of a pure solution. Carroll and Lucassen[25] pulled a fiber through an oil–water interface, in the presence of the surfactant tetradecyl trimethyl ammonium bromide, and observed that the film was about 2.5 times thicker than the pure fluid case (they worked with capillary numbers $2\times10^{-3}\leqslant\mathcal{C}\leqslant0.1$). Similarly, Quéré and coworkers reported that the film tends to thicken when SDS is present in the solution compared to that of a pure solution.[2,3,9]

Here we report experiments using a series of binary fluid systems, consisting of mixtures of distilled water with a single surfactant, and investigate how different bulk concentrations of surfactant alter the film thickness for three different types of surfactants. In particular, we tested the film thickness response towards very high surfactant concentrations and demonstrate that even though surfactant additives generally tend to thicken the coating film, at elevated bulk concentrations the sorption kinetics of different surfactants can play a key role in the determination of the film thickness.

C. Thickening factor for surfactant solutions

Before presenting our experimental results, we introduce the concept of the thickening factor, which is useful for characterizing the influence of surfactants. We define the thickening factor α as the ratio of the measured film thickness h of a fluid with surfactant to the film thickness predicted by the LLD relation:

$$\alpha=\frac{h}{h_{\mathrm{LLD}}}=\frac{h/b}{1.34\mathcal{C}^{2/3}}. \tag{7}$$

The capillary number $\mathcal{C}$ is calculated by using the static surface tension value γ for the surfactant solution, i.e., the value of γ corresponding to the equilibrium surface tension with the specified bulk concentration. Ideally, for a clean Newtonian fluid, $\alpha=1.0$.

As described previously, the presence of surfactants tends to thicken the film during the course of fiber coating due to a surface tension gradient. Carroll and Lucassen[25] first reported this trend experimentally (though it was also indicated in an early publication by Bretherton[6]) and they found that the thickening factor is approximately $\alpha=2.5$. Recently, Quéré and de Ryck[9] performed fiber-coating experiments with SDS at concentrations $0.01\leqslant\phi\leqslant10$ and found that $1.0\leqslant\alpha\leqslant2.2$. We compare their results with our measurements below.

D. Micellar stability

Micelles appear when the surfactant concentration reaches a critical value, the CMC. The micelles are in dynamic equilibrium and so are continuously disintegrating and reforming in solution. There are two major time scales involved. The first process is relatively fast, associated with the individual monomers exchanging from solution into a micelle, while there is a much slower second time scale on which the micelle either forms or completely disintegrates.[21] It is this second slow time scale that is rate limiting when considering the role of the micelle as a surfactant source adjacent to an interface that is being stretched. The stability of the micelle depends on the bulk concentration because of micelle–micelle interactions that involve the intermicellar distance, and is also strongly influenced by Coulombic effects that are expected to be larger for ionic surfactants. More stable micelles imply that the monomer flux between the micelles and the bulk solution is decreased and consequently the ability of micelles to act as monomer sources, which can replenish the stretching interface, is diminished. In other words, the dynamic surface tension, which generates the Marangoni flow, is dependent on micelle stability. The experimental results reported in Sec. IV C appear consistent with the idea that the dynamics of fiber coating can be influenced by the stability of micelles for $c>\mathrm{CMC}$.[21]

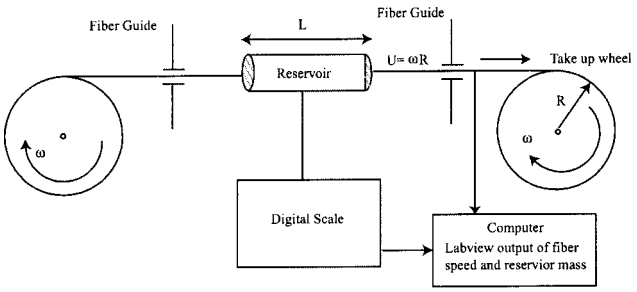

FIG. 2. Sketch of the experimental setup. The film thickness is determined by monitoring the mass loss from the fluid-filled reservoir.

III. EXPERIMENTAL SETUP AND PROCEDURE

We are interested in the coating thickness on a fiber as it is pulled at various speeds through a fluid bath with surfactant additives. For each fixed amount of bulk surfactant concentration, we vary the fiber speed slowly and measure the film thickness accordingly. The determination of the thickness of the entrained fluid film on a fiber is based on the configuration utilized by de Ryck and Quéré;[8] see Fig. 2.

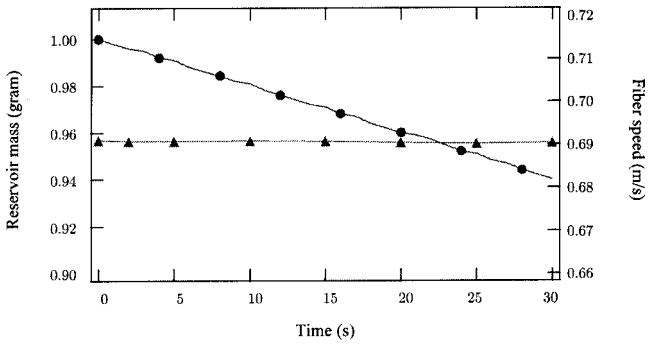

FIG. 3. Experimental data of reservoir mass (left ordinate) and fiber speed (right ordinate) versus time. Every fourth data point is indicated by a symbol. SDS solution (0.2% by weight) with fiber speed 0.69 m/s.

Downloaded 03 Jan 2003 to 18.80.1.86. Redistribution subject to AIP license or copyright, see http://ojps.aip.org/phf/phfcr.jsp

TABLE I. Fluid properties of BSA solution at different bulk concentrations.

Bulk concentration c (weight percentage %)	$\phi^*=c/c^*$, $c^*=0.001\%$ at which multilayers form	Viscosity μ (10^{-3} N·s/m^2)	Equilibrium surface tension γ (N/m)
0.0001	0.100	1.0	0.0689
0.0005	0.500	1.0	0.0688
0.001	1.00	1.0	0.0688
0.004	4.00	1.0	0.0688
0.025	25.0	1.0	0.0676
0.05	50.0	1.0	0.0676
0.16	160	1.0	0.0611

Instead of measuring the film thickness directly by visualization, we use an indirect but accurate technique. A single-strand fiber is pulled from a spool through a horizontal fluid-filled Teflon tube (McMaster–Carr) to a take-up wheel (14 cm in diameter) rotated by a dc motor. The Teflon tube, with an internal diameter of 0.5 cm and length of 3.5 cm, contains a few liquid drops (~ 40 μL) of the solutions to be coated onto the fiber and is positioned in the center of a digital mass balance (Sartorius AG-D37070).

The fiber is a thin steel wire (from Spring Temper) with radius $b=0.038\pm 0.002$ mm. As the fiber passes through the fluid-filled reservoir, the mass of the reservoir decreases due to coating of the fiber. The mass of the reservoir and the fiber speed are both recorded digitally using the LabView data acquisition program. The change in mass δm of the fluid in the Teflon tube recorded during an elapsed time δt is related to the uniform film thickness h on a fiber of radius b by

$$\delta m=\rho\pi U\delta t(h^2+2hb)\Leftrightarrow\frac{h}{b}=\sqrt{1+\frac{\delta m}{\rho\pi Ub^2\delta t}}-1. \tag{8}$$

In particular, our experimental measurements show that for small capillary numbers, the slope $\delta m/\delta t$ is nearly constant (see Fig. 3), which in turn indicates that the film thickness is a constant with respect to time.

All experiments were performed at an ambient temperature of 25 °C. Solutions were filtered and made fresh daily to ensure purity and the Teflon reservoir was changed for each solution. Further, all reported results below are reproducible as data for all concentrations was taken multiple times and on multiple days. The surface tension of each solution was measured using a Wilhelmy plate in a Krüss K-10 tensiometer and the static surface tension was taken as the value when the measurement reached steady state. Typically, the surface tension for aqueous surfactant solutions range between 0.03 N/m (at high surfactant concentration) and 0.072 N/m (nearly clean system). We used a TA Instruments AR1000N stress controlled rheometer to measure the viscosity of the fluids. Since the fluids used were water-based solutions with surfactants, their viscosities were very close to the value $\mu_w=1.0029\times 10^{-3}$ Pa·s for water at 25 °C (except for very high concentrations of SDS which slightly elevated the viscosity). The densities of each fluid were also nearly identical to that of pure water.

We also take into account that some evaporation of fluid of mass δm^* during time δt may occur during the coating process. We use a slightly modified version of Eq. (8) to account for this effect:

$$\frac{h}{b}=\sqrt{1+\frac{(\delta m-\delta m^*)}{\rho\pi Ub^2\delta t}}-1. \tag{9}$$

Measurements were made to determine δm^*, but as $\delta m^*/\delta m\ll 1$, the evaporation of the solution, was not important in our experiments.

We collected data for the film thickness versus the capillary number for each surfactant type in the following manner: we fixed an initial amount of surfactant in the bulk solution (distilled water), mixed the solution well, placed it in the reservoir on the balance, increased the fiber speed to a

TABLE II. Fluid properties of Triton X-100 solution at different bulk concentrations.

Bulk concentration c (weight percentage %)	$\phi=c/\mathrm{CMC}$, $\mathrm{CMC}=0.016\%$ at which micelles form	Viscosity μ (10^{-3} N·s/m^2)	Equilibrium surface tension γ (N/m)
0.001	0.0625	1.0	0.0498
0.004	0.250	1.0	0.0365
0.007	0.438	1.0	0.0325
0.01	0.625	1.0	0.0315
0.02	1.25	1.0	0.0310
0.024	1.50	1.0	0.0310
0.029	1.80	1.1	0.0310
0.04	2.50	1.2	0.0310
0.08	5.00	1.3	0.0310
0.22	13.8	1.3	0.0310
1.02	63.8	1.4	0.0310
4.0	250	1.5	0.0310
10	625	1.7	0.0310

Downloaded 03 Jan 2003 to 18.80.1.86. Redistribution subject to AIP license or copyright, see http://ojps.aip.org/phf/phfcr.jsp

TABLE III. Fluid properties of SDS solution at different bulk concentrations.

Bulk concentration c (weight percentage %)	$\phi = c/\mathrm{CMC}$, CMC = 0.24% at which micelles form	Viscosity μ (10^{-3} N·s/m^2)	Equilibrium surface tension γ (N/m)
0.01	0.0420	1.0	0.0565
0.03	0.125	1.0	0.0514
0.05	0.208	1.0	0.0464
0.1	0.420	1.0	0.0394
0.2	0.840	1.0	0.0384
0.3	1.25	1.0	0.0380
0.7	2.92	1.0	0.0375
1.2	5.00	1.1	0.0371
2.0	8.33	1.2	0.0370
4.0	16.7	1.4	0.0356
5.7	23.7	1.5	0.0351
12.0	50.0	3.2	0.0350
20.0	83.3	3.6	0.0350

constant value for a certain period of time during which the mass of fluid within the reservoir was measured by the digital balance, then incremented the speed to another constant value and repeated the same mass measurement. The corresponding values of capillary numbers were evaluated using data given in Tables I–III. In particular, the surface tension value being used when reporting results in terms of the capillary number is the equilibrium value for the static state. We also define a dimensionless parameter ϕ characterizing the bulk concentration of surfactant as $\phi = c/\mathrm{CMC}$; note that for BSA the CMC is replaced by the critical concentration c^* at which multilayers form on the interface. Thereafter, we varied the bulk concentration and repeated the procedure described above, until the bulk surfactant concentration attained values as high as 625 times the critical micelle concentration.

IV. EXPERIMENTAL RESULTS

A. Coating results for Newtonian fluids

To verify the accuracy of the experimental setup and measurement technique, we selected deionized water and a 35 wt% glycerin in water mixture as test fluids for the fiber coating. The glycerin/water mixture has a surface tension $\gamma = 0.072$ N/m, density $\rho = 1000$ kg/m^3, and viscosity $\mu = 2.9\times10^{-3}$ N·s/m^2. The coating thickness h scaled by the fiber radius b should be proportional to $\mathcal{C}^{2/3}$ based on the LLD relation. Figure 4 shows that over a moderate range of $\mathcal{C}$, the experimental data fits very well with the LLD equation (4), as shown by the solid line. However, we observed some discrepancy at very small and large capillary numbers: at very small $\mathcal{C}$, the fluid barely wets the fiber, so the coating thickness is much smaller than the predicted value, while at higher speeds, due to inertial effects, the film thickness exceeds the value predicted by the LLD relation (see the detailed discussion in Quéré and de Ryck[8]).

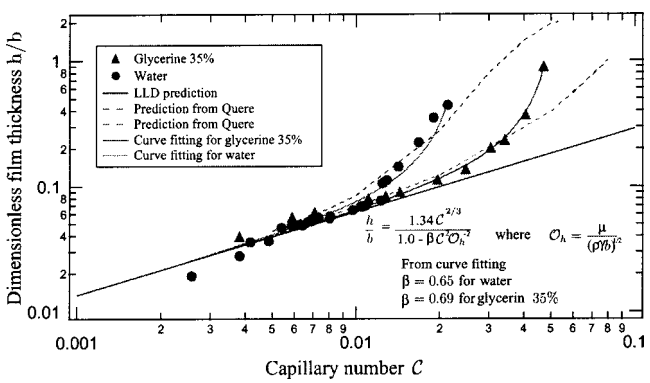

FIG. 4. Film thickness versus capillary number for a solution of 35% glycerin by weight in a water solution and for pure water. The solid lines are the best fit using Eq. (5). The dotted lines are obtained using Eq. (6).

The rapid thickening of the film beyond the LLD region is due to inertial effects in the fluid and can be described using Eq. (5). We find that $0.65 \leqslant \beta \leqslant 0.69$ fits the two sets of experimental data well, as shown in Fig. 5. A second approximate procedure for determining β was developed by de Ryck and Quéré;[23] see Eq. (6), where β depends on the film thickness h and the radius of the fluid reservoir. We also made comparisons of (6) with our data, as plotted in Fig. 4. There appears to be reasonable agreement.

B. Coating results for surfactant solutions

We will present fiber-coating results for experiments using three different surfactants: the protein BSA, the nonionic surfactant Triton X-100, and the anionic surfactant SDS. The experimental results for these different systems have some similarities, owing to physical responses expected due to capillary effects and Marangoni stresses, as well as some differences largely due to the different kinetic rates of each surfactant system. These issues will be discussed individually for the data on each system.

1. Protein BSA

The surface active protein bovine serum albumin (BSA) was purchased from Sigma in a powder form and mixed with distilled water. BSA does not form micelles. Instead, the desorption rate is very slow, and the protein denatures on the interface. Also, BSA tends to form multilayers on the interface[16,26] and it is known that BSA is negatively charged at neutral pH. Material properties for BSA are reported in Table I.

Downloaded 03 Jan 2003 to 18.80.1.86. Redistribution subject to AIP license or copyright, see http://ojps.aip.org/phf/phfcr.jsp

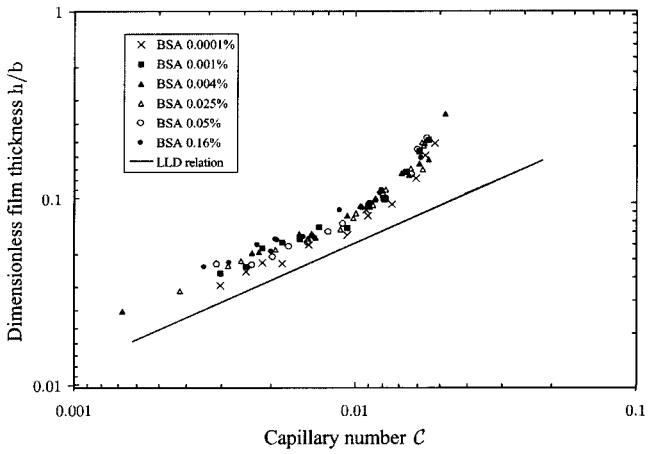

FIG. 5. Dimensionless film thickness versus capillary number for various bulk concentrations of BSA.

The concentration of BSA was varied between $0.01 \leqslant \phi^* \leqslant 160$, where $\phi^* = c/c^*$ with c^* equal to the concentration at which multilayers form on the fluid surface.[26] In Fig. 5, we plot the dimensionless film thickness h/b against the capillary number and compare the experimental data with the LLD result (solid line); for clarity, only half of the data we obtained for different bulk concentrations is shown. For a range of capillary numbers, at each fixed bulk concentration, the data for the film thickness is almost parallel to, but above, the LLD relation (solid line), implying that the thickening factor is essentially independent of the capillary number. This feature is important since it allows for a simple characterization of the film thickening as a function of surfactant concentration according to the thickening factor α, Eq. (7). An explanation for this dependence, which is consistent with α being independent of speed, may be based on a consideration of dynamical and kinetic rates, as discussed by Quéré *et al.*;[2] see also Sec. VI.

The thickening factor as a function of the bulk surfactant concentration is shown in Fig. 6, where the thickening factor is taken as the average value in the region parallel to the LLD solid line in Fig. 5. The data in Fig. 6 show that the coating thickness for BSA quickly reaches a maximum at a very small concentration $c \approx c^* = 0.001\%$ by weight. We denote this as regime I, in which Marangoni stresses promote

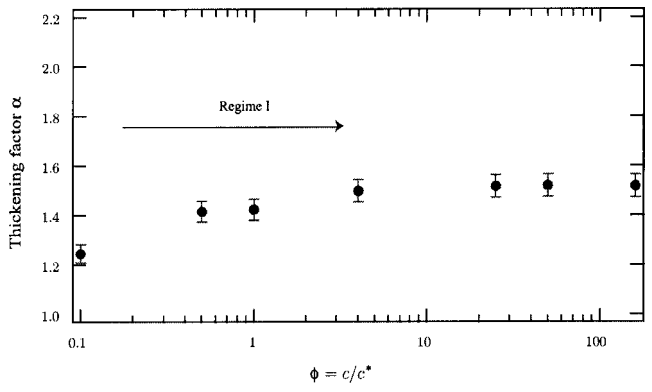

FIG. 6. Thickening factor α vs $\phi = c/c^*$ for BSA solutions. The concentration c^* is where multilayer formation begins.

the film thickening. Thereafter, the film thickness is approximately a constant for continuously increasing bulk concentration and we denote this second region as regime II.

It is interesting to note that the saturated value of the thickening factor is approximately $\alpha \approx 1.5 \approx 2^{2/3}$, which agrees well with Bretherton's theoretical prediction[6] based upon the idea that the free surface is at rest. Nevertheless, this interpretation is not consistent with the manner in which the film thickness is deduced from the mass-loss measurement, since the measurement assumes a film with a uniform velocity profile rather than the linear shear profile expected if the interface was at rest. Instead, we believe that the saturated value of α that is observed is a result of rheological properties of the film. Since the desorption rate for BSA is very slow, when BSA monomers adsorb/transport onto the interface, the monomers simply accumulate there and when the surfactant concentration reaches some critical value, the surface behaves like a viscous (or possibly viscoelastic) interface.[26] Therefore, the adsorbed BSA on the surface never becomes mobile at high bulk concentrations, as is common for smaller surfactants, so that the remobilization regime observed with the other surfactant systems (discussed further below) is never realized for this surfactant.

It is possible that surface rheology impacts the data reported for BSA solutions. We measured the surface viscosity of BSA using a CIR-100 interfacial rheometer from Camtel/Rheometric Scientific and obtained surface viscosity $\mu_s = 2.6$ mN·s/m (measurements were taken at frequency 3 Hz and a BSA concentration 0.025%). Since $\mu_s/\mu h \simeq 10^6$, this suggests that surface rheology likely contributes to the observed coating response.

2. Triton X-100

The second system we studied is the nonionic polyethoxy surfactant, Triton X-100, whose chemical formula is $CH_3C(CH_3)_2CH_2C(CH_3)_2C_6H_4E_nOH$, where n is between 9 and 10. We purchased Triton X-100 from Aldrich in liquid form. The critical micelle concentration for this surfactant is 0.016% by weight.[16] The concentration of Triton X-100 ($\phi = c/\mathrm{CMC}$) was varied between $0.06 \leqslant \phi \leqslant 625$. Fluid properties for this solution are listed in Table II.

Figure 7 shows the dimensionless film thickness h/b as a function of the capillary number, while the bulk concentration of Triton X-100 is varied systematically. Again, this figure only selects half of the data sets we obtained and the solid line in the figure represents the LLD prediction. For a range of capillary numbers, the film thickness is almost parallel to, but above the LLD relation (solid line) for each fixed bulk concentration and we take the thickening factor as the average value over this linear range. The thickening factor is plotted in Fig. 8 where we observe that, well below the CMC, the film thickness increases monotonically with increasing bulk concentration (regime I), which is consistent with the physical argument of the Marangoni effect. When the concentration is somewhat above the CMC, α decreases slightly (region II), but beyond a narrow range of concentrations, the film thickness increases again, finally saturating at $\alpha \simeq 1.75$ at the highest concentration we measured.

Downloaded 03 Jan 2003 to 18.80.1.86. Redistribution subject to AIP license or copyright, see http://ojps.aip.org/phf/phfcr.jsp

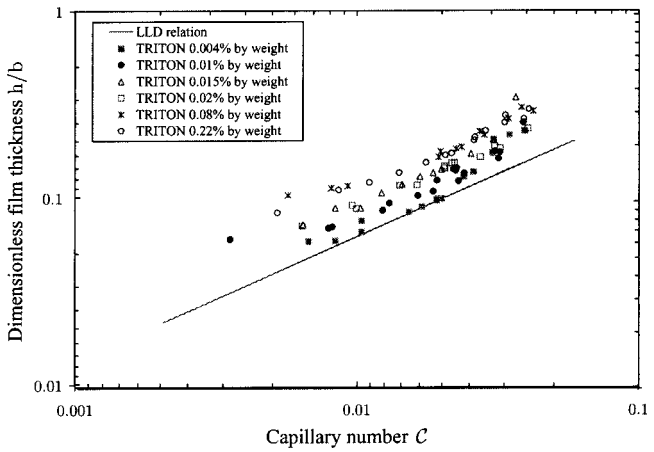

FIG. 7. Dimensionless film thickness versus capillary number for various bulk concentrations of Triton X-100.

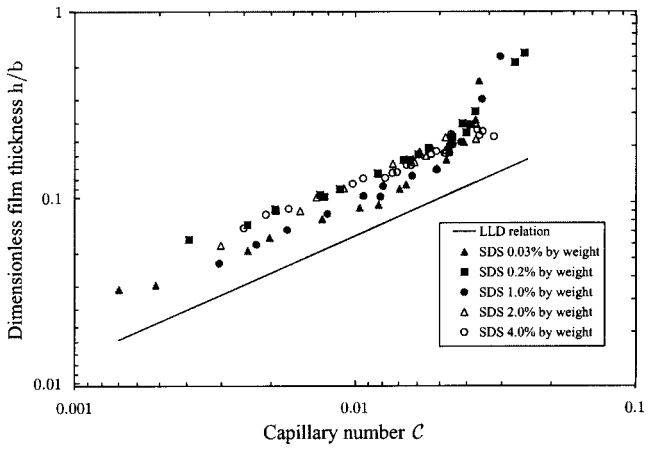

FIG. 9. Dimensionless film thickness versus capillary number for various bulk concentrations of SDS.

Here, we believe that the decrease of the film thickness in the neighborhood of the CMC can be explained by the mechanism of surface remobilization, as elucidated by Stebe *et al.*[16] When the bulk concentration exceeds the CMC, there are micelles present in solution. As the micelles are in dynamic equilibrium with free surfactant monomers in the bulk solution, monomers are constantly being exchanged with the micelles, and so micelles close to the interface can act as reservoirs of free monomers. Hence, the surfactant distribution on the interface becomes more uniform as compared to the situation with $c<$CMC. As a consequence the surface tension gradient decreases and therefore the thickening factor α decreases. Thus, we refer to regime II as the surface remobilization region. However, the experimental results clearly show that with further elevation in bulk concentration, the film thickness increases once more and then saturates to a constant value at $3\leqslant\phi\leqslant625$ (regime III). We shall discuss below a possible explanation for this additional thickening, since a similar effect is also observed with SDS, as discussed next.

C. SDS

Sodium dodecyl sulfate (SDS: $C_{12}H_{25}OSO_3Na$) is an anionic surfactant and was purchased from Aldrich in a powder form. The concentration of SDS ($\phi=c/$CMC) was varied between $0.01\leqslant\phi\leqslant85$. The fluid properties for these solutions are reported in Table III. There was no measurable surface viscosity when all solutions were tested using the CIR-100 interfacial rheometer from Camtel/Rheometric Scientific.

In Fig. 9, we plot the dimensionless film thickness against the capillary number for $\phi<20$ and compare the experimental data with the LLD result (solid line). As in previous figures, the thickening factor is taken as the average value in the region parallel to the LLD solid line in Fig. 9. A complete illustration of the thickening factor with respect to the bulk surfactant concentration is shown in Fig. 10. We have also included the data obtained by Quéré and coworkers[2] for the same surfactant system, though their data covers a somewhat smaller concentration range for coating on a molybdenum wire with radius equal to 12.5 μm. Although there are some quantitative differences, the basic trends of our observations are consistent with their results.

In Fig. 10, we notice that at very low concentrations, barely any film thickening is observed. However, the thickening effect becomes significant when the concentration exceeds $\phi\geqslant0.03$. In particular, just below the CMC, the thickening factor reaches a first maximum $\alpha\simeq2.029$ with $\phi\simeq0.4$. The film thickening in this monotonically increasing part of the data (regime I), up to concentrations just below

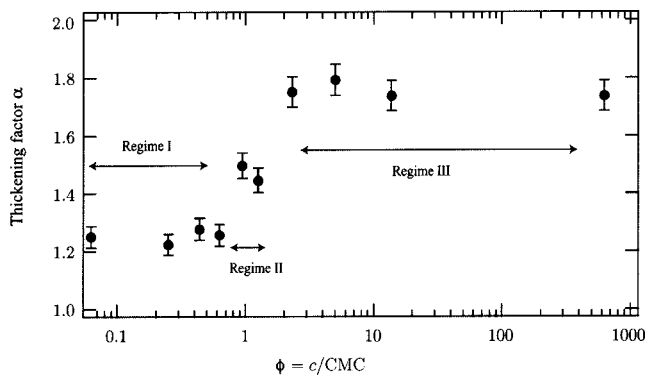

FIG. 8. Thickening factor α vs $\phi=c/$CMC for Triton X-100 solutions.

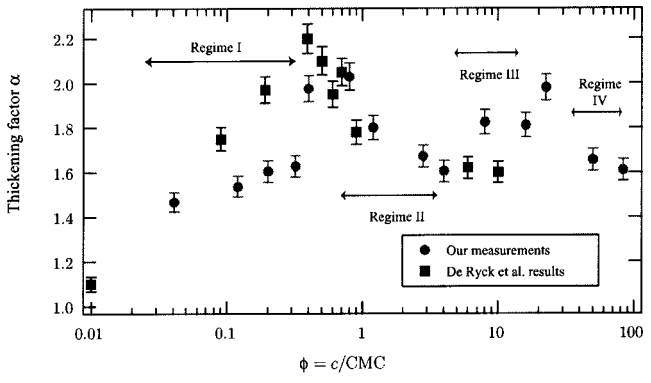

FIG. 10. Thickening factor α vs $\phi=c/$CMC for SDS solutions.

Downloaded 03 Jan 2003 to 18.80.1.86. Redistribution subject to AIP license or copyright, see http://ojps.aip.org/phf/phfcr.jsp

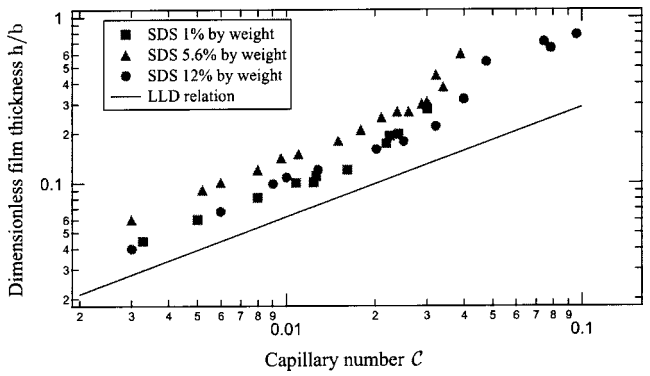

FIG. 11. Dimensionless film thickness versus capillary number for SDS at very high concentrations.

the CMC, is consistent with the Marangoni-induced flow toward the film due to a surface tension gradient in the meniscus region.

Further, as the bulk concentration surpasses the CMC, α begins to decrease with increasing concentration, which we indicate as regime II. Regimes I and II were also observed by Quéré[3] for this surfactant. Note that this remobilization regime II is much wider in extent than that present in the case of Triton X-100 (Fig. 8). This decrease in α is consistent with a surface remobilization effect, as was also argued in slightly different terms by Quéré and coworkers.

We have also made observations when the bulk concentration is much higher than the CMC, which, to the best of our knowledge is a limit which has not been studied before in the fiber-coating configurations. The scaled film thickness, h/b, for these higher concentrations is plotted versus capillary number in Fig. 11. The second maximum in the thickening factor α shown in Fig. 10 is also evident when the data is plotted directly as the scaled film thickness h/b. When $\phi \simeq 10$, the film once again starts to thicken to a second maximum until the bulk concentration reaches $\phi \simeq 25$. We refer to this region as regime III and note that, qualitatively, a thickening response like this was also observed in the Triton data. Moreover, as we continue to increase the bulk concentration even further, $\phi > 25$, the dimensionless film thickness decreases and eventually reaches a value $\alpha \simeq 1.6$ (regime IV) for the highest concentrations we studied. The above behavior demonstrates that the sorption kinetics of SDS have a direct impact on the film thickness.

It is possible to understand, at least qualitatively, the trends of coating thickness as a function of bulk surfactant concentration, in particular the second maximum at high concentrations of SDS. The initial increase of α with ϕ, followed by a decrease near the first maximum in Fig. 10 at $\phi \simeq 0.5$ corresponds to the Marangoni-induced thickening and subsequent remobilization associated with the presence of micelles as sources of surfactant. However, we observe a second maximum in the plot of α vs ϕ. Here we note that basic physicochemical measurements have recently shown that a maximum micellar stability occurs at $\phi \simeq 25$ ($c = 200$ mM);[21,22] in other words, the kinetics associated with micelle–monomer exchange of this ionic surfactant are dependent on the bulk concentration of surfactant. To a very good approximation, this concentration $c = 200$ mM is where the second maximum in coating thickness is observed in Fig. 5 (see the discussion in Sec. V and Fig. 13). The second maximum is followed by a further surface remobilization as the micelle stability decreases at higher concentration when $\phi > 25$.

We conclude this section with a short summary of some aspects of micelle stability since it seems so closely linked with the second maximum in the film thickening factor α as a function of concentration, and so provides a direct link between physicochemical characteristics and dynamic measurements. We believe that our observation of a second maximum in coating thickness α as a function of $\phi = c/\mathrm{CMC}$, and its relation to micelle stability, as described by Shah and coworkers,[21,22] has not been pointed out before.

As the concentration of SDS is increased further ($\phi > 25$), equilibrium measurements show that there is a structural transition from spherical to cylindrical micelles to accommodate more surfactant molecules in the solution.[21] This (phase) transition produces micelle structures that are less stable relative to the spherical shape and so the rate of exchange between the surfactant structures and bulk monomers is increased. Consistent with this idea, we observe that the coating thickness falls into a second surface remobilization regime, which we have labeled regime IV. It is of course also possible that these structural changes produce a bulk non-Newtonian rheological response of the surfactant solution, which could then be related to the experimentally observed second maximum, see Fig. 10. The shear rates in the fiber coating experiments are beyond those accessible in standard rheometers. For example, in the neighborhood of the stagnation point along the surface, the shear rate is approximately $\dot{\gamma} \simeq U/h \simeq U/b\mathcal{C}^{-2/3} \simeq 10^5\ \mathrm{s}^{-1}$. We have not been able to investigate this rheological mechanism further.

V. DISCUSSION

We have measured the film thickness during fiber coating for different surfactant solutions and find different responses of the film thickness as a function of concentration, especially as the concentration approaches and goes beyond the CMC (or multilayer formation in the case of BSA). Data for the film thickening factor α as a function of (normalized) surfactant concentration are compared directly in Fig. 12. There are common qualitative trends in the data which we labeled regimes I–IV in earlier graphs. In particular, the thickening behavior shows additional structure for SDS and Triton X-100 at high concentrations. These observations indicate that sorption/desorption kinetics and the stability characteristics of micelles for each individual surfactant system play important roles in the establishment of the usual capillary and Marangoni-induced flows and so impact the film thickness during coating.

For all three surfactants the film thickens with increasing surfactant concentration (for concentrations below the critical micelle concentration). The thickening is a consequence of (i) a lower surface tension, which decreases the usual capillary suction out of the film, and (ii) a Marangoni-induced flow, due to the surface tension gradient in the re-

Downloaded 03 Jan 2003 to 18.80.1.86. Redistribution subject to AIP license or copyright, see http://ojps.aip.org/phf/phfcr.jsp

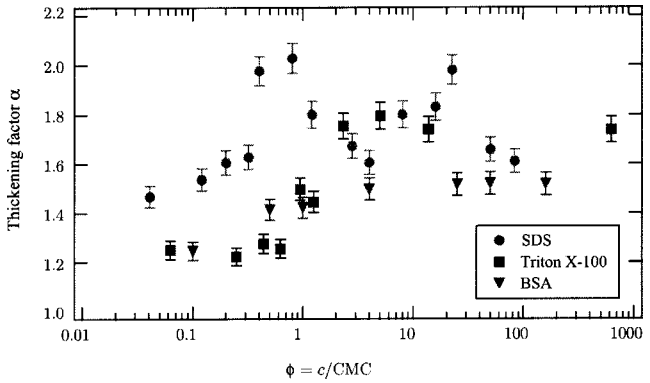

FIG. 12. Thickening factor α for three surfactants BSA, Triton X-100, and SDS. For BSA interpret the CMC as the concentration at which multilayers form.

gion of the meniscus, which drags fluid from the bath into the film. We observe that the thickening factor [Eq. (7)] is a function of the bulk concentration but not the capillary number; this fact was first demonstrated by Quéré and coworkers[2] and explained on the basis of estimates showing that the typical time for convection through the meniscus region scales with capillary number in a similar manner as adsorption processes (discussed further below). When the bulk concentrations exceed the CMC, the film thickness decreases for both SDS and Triton X-100 apparently due to a surface remobilization mechanism, analogous to the description of this process given by Stebe *et al.*[16] The remobilization regime was not observed for the protein BSA most likely owing to rheological effects of the surface multilayers associated with this higher molecular weight surfactant. Furthermore, at very high bulk concentrations, the behavior of the film thickness for SDS shows a second maximum, while that for Triton X-100 increases and then saturates. At these higher concentrations the relative rates of formation and disintegration of the micelles (i.e., the micellar stability) are a function of the bulk surfactant concentration and this introduces an additional kinetic time scale that influences the dynamics of the coating flow. The concentration at which this second maximum occurs is consistent with independent physical chemistry measurements of a micellar lifetime made with SDS.[21,22] Furthermore, recent experimental work has provided evidence that the structure and rheology of surfactant-laden complex fluids can change significantly at high shear rates comparable to those encountered in the present experiments.[27,28]

To understand the observed trends it is necessary to characterize both the dynamics and kinetics of the process, which involve many potentially important time scales. In Table IV we provide a list of the most important time scales and, where possible, give some rough estimates for their typical order of magnitude. Although we have not succeeded in developing a complete theory for the influence of chemical kinetics on fiber coating, we consider the information in the table and the brief discussion below to be important in formulating a complete theory. For a discussion of modeling that includes kinetic effects, see Schunk and Scriven.[1]

We discuss three time scales related to convection, diffusion, and adsorption/desorption of surfactants during fiber coating.

(I) There is a well-defined convective time scale t_c that characterizes the time necessary for a typical surface material element to move through the dynamic meniscus. It is estimated as

$$t_c \sim \frac{\ell}{U} = \frac{b\mathcal{C}^{1/3}}{U} = \frac{b\mu}{\gamma}\mathcal{C}^{-2/3} = \left(\frac{b^3\mu}{\gamma U^2}\right)^{1/3}, \tag{10}$$

with U the fiber speed, b the fiber radius, and ℓ the characteristic length scale along the fiber evaluated within the LLD mathematical framework (e.g., see the Appendix).

A closely related time scale of possible importance is the rate of stretching of surface material elements. Denoting the surface velocity as u_s and the distance along the interface as s, then the inverse of the rate of stretching is $t_{\mathrm{str}} \sim 1/|du_s/ds|$. Using standard results from the analyses of fiber coating (e.g., Quéré[3] or the Appendix), $t_{\mathrm{str}} \sim (b\mu/\gamma)\mathcal{C}^{-2/3}$. The ratio of these two time scales deter-

TABLE IV. Important time scales and dimensionless groups for different surfactants under fiber coating. The characteristic values for SDS and Triton X-100 are taken from Chang and Franses (Ref. 29) and Fdhila and Duineveld (Ref. 30). The protein data are taken from Graham and Phillips (Ref. 26) and Miller *et al.* (Ref. 31). For the adsorption time scale, $t_{\mathrm{ad}} = 1/(k_a c)$, we used $c = \mathrm{CMC}$ for the calculation. However, for higher concentrations, the adsorption rate is lower; see the discussion.

Surfactant	SDS	Triton	BSA
Critical concentration by weight	0.24%	0.016%	0.001%
Maximum surface concentration Γ_m (10^{-6} mol/m^2)	10	2.9	4.64×10^{-6}
Diffusion coefficient D (10^{-10} m^2/s)	8	2.6	1
Adsorption coefficient k_a (m^3/s·mol)	333	50	0.735
Desorption coefficient k_d (s^{-1})	25	0.033	10^{-6}
Convective time scale $t_c = \ell/U$ (10^{-4} s)	(0.04,1)	(0.04,1)	(0.04,1)
Diffusion time scale along the fiber, $t_{d1} \sim \ell^2/D_s$ (s)	(0.02,0.08)	(0.06,0.25)	(0.16,0.64)
Diffusion time scale from bulk to the surface, $t_{d2} \sim h^2/D$ (s)	2.0	6.2	16.0
Diffusion time scale of adsorption depth, $t_{d3} \sim (\Gamma_m/c)^2/D$ (s)	0.002	0.611	0.096
Adsorption time scale $t_{\mathrm{ad}} = 1/(k_a c)$ (s)	$\simeq 0.0004$	$\simeq 0.087$	$\simeq 9\times10^3$
Desorption time scale $t_{\mathrm{de}} = 1/k_d$ (s)	0.04	30	10^6
Micelle disintegration time t_m (s)	(10^{-4},10)	(3,5)	N/A
t_c/t_{ad}	(0.01,0.25)	(4×10^{-3},0.1)	(4×10^{-10},10^{-8})

Downloaded 03 Jan 2003 to 18.80.1.86. Redistribution subject to AIP license or copyright, see http://ojps.aip.org/phf/phfcr.jsp

mines the strain ϵ experienced by a surface material element, $\epsilon = t_c/t_{\rm str} = O(1)$, which may be important for those cases where surface rheology matters. We also note, however, that there is a stagnation point along the surface so that surface material elements move *slower* than the estimate given in (10). For a clean interface the velocity varies linearly with distance from the stagnation point and so the convective time is increased from (10) by a factor $\ln(\ell/\Delta)$ where $\ell = b\mathcal{C}^{1/3}$ is the typical length of the dynamic meniscus (see the Appendix) and Δ is a small cut-off length scale, say the typical size of a surfactant molecule. This effect of a surface stagnation point increases the estimate of the convective time scale by approximately a factor of 10.

(II) The characteristic time scales for surfactants to diffuse along the meniscus t_{d1}, diffuse through the film thickness t_{d2}, or simply diffuse through the surfactant adsorption depth $\ell_\perp = \Gamma_m/c$ of the sublayer region t_{d3},[32] are

$$t_{d1} = \frac{\ell^2}{D_s} = \frac{b^2}{D_s}\mathcal{C}^{2/3}, \quad t_{d2} = \frac{h^2}{D} = \frac{b^2}{D}\mathcal{C}^{4/3},$$

and

$$t_{d3} = \frac{\ell_\perp^2}{D} = \frac{\Gamma_m^2}{Dc^2}. \tag{11}$$

Here D is the bulk diffusion coefficient, D_s the surface diffusion coefficient, and Γ_m is the maximum surface concentration of surfactant. Further, D and D_s may change when the bulk concentration c exceeds the CMC. It is not clear whether the values for the diffusion coefficients listed in Table IV are valid for very high surfactant concentrations.

(III) The time scales for adsorption $t_{\rm ad}$ and desorption of the surfactant $t_{\rm de}$ between the bulk solution and the interface may be estimated as

$$t_{\rm ad} = \frac{1}{k_a c} \quad \text{and} \quad t_{\rm de} = \frac{1}{k_d}, \tag{12}$$

with k_a the surfactant adsorption coefficient and k_d the surfactant desorption coefficient; this estimate for $t_{\rm ad}$ is common for low bulk surfactant concentrations. Again, the adsorption and desorption coefficients k_a and k_d may be functions of the surfactant concentration. Most importantly, Eq. (12) makes clear that the adsorption rate increases as the bulk concentration increases.

When adsorption occurs at a highly covered interface the adsorption rate is reduced due to molecular crowding on the interface, hence the rate may be estimated as $\tilde{t}_{\rm ad}^{-1} = k_a c(\Gamma_m - \Gamma)/\Gamma_m$, where the surface concentration $\Delta\Gamma = \Gamma_m - \Gamma$ is related to the Marangoni stresses that influence surface flow. The change in surfactant concentration $\Gamma_m - \Gamma = \Delta\Gamma \propto \Delta\gamma$, which in turn can be estimated from the magnitude of Marangoni stresses tangential to the surface: $\Delta\gamma \propto \mu U\ell/h \propto U^{2/3}$. We thus see that $\tilde{t}_{\rm ad} \propto U^{2/3}$ and consequently $t_c/\tilde{t}_{\rm ad}$ is independent of speed. This argument was given by Ramdane and Quéré[9] and is consistent with the experimental observation that the film thickening factor α is independent of speeds. The implication of this estimate is that at higher concentrations, where $\Gamma \to \Gamma_m$, the adsorption rate can be significantly lower than $t_{\rm ad}$.

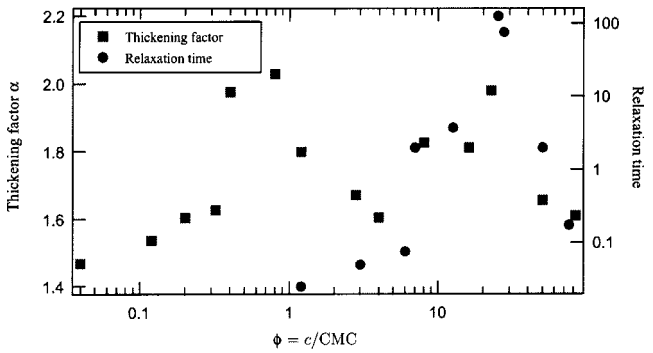

FIG. 13. The thickening factor (squares) for SDS plotted as a function of concentration and overlayed with the data for micelle lifetime (circles) for SDS obtained by Patist *et al.* (Ref. 21).

In the experiments reported here, the fiber radius $b = 0.038$ mm and the fiber speed $0.1 \leqslant U \leqslant 3$ m/s, so the capillary numbers are $0.001 \leqslant \mathcal{C} \leqslant 0.1$. We also assume that the surface diffusivity coefficient is similar to the bulk value, so $D_s \sim 10^{-10}$ m^2/s. By using these parameters, we provide in Table IV estimates for the above mentioned time scales.

The values in Table IV can then be used to understand the evolution in the thickening factor over the entire range of concentrations studied.

(i) For low concentrations ($\phi < 1$), the motion of surfactant molecules from the bulk to the interface can be considered as a three step process; diffusion through the bulk (t_{d2}), diffusion across the adsorption sublayer (t_{d3}) and finally adsorption onto the interface ($t_{\rm ad}$). It is clear from the consideration of Table IV that for the Triton and SDS surfactants considered in this study, this process is *diffusion-controlled* and the Damkohler number $\mathrm{Da} = t_{d2}/t_{\rm ad} \gg 1$ [see (II) above].

(ii) As the concentration increases beyond the CMC, a fourth process becomes important; the generation of surfactant monomer from the micellar aggregates. Provided the micellar lifetime (here denoted $t_{\rm micelle}$) is short, so that there is rapid exchange of individual monomers in and out of micelles, then the migration of monomers to the interface will still be limited by diffusion through the bulk (i.e., $t_{\rm micelle} \ll t_{d2}$). The large, nearly uniform surface coverage of surfactant will result in low equilibrium values of surface tension but also low values of the surface tension gradients and, hence, the interface may be remobilized.[16,19]

(iii) However, if the micellar lifetime increases so that $t_{\rm micelle} \sim t_{d2}$, then the replenishment of surfactant molecules on the interface will be controlled not just by diffusion through the bulk, but also by the dynamic equilibrium between the number of free surfactant monomers in the bulk and in the micelles. For the anionic surfactant SDS, recent measurements[21] using a variety of techniques, including fluorescence decay, show that the typical micellar lifetime $t_{\rm micelle}$ can increase by several orders of magnitude up to $\phi \sim 25$. The time scales for disintegration vary from 10^{-3} seconds at $c/\mathrm{CMC} = 3$ to about 5 seconds at

Downloaded 03 Jan 2003 to 18.80.1.86. Redistribution subject to AIP license or copyright, see http://ojps.aip.org/phf/phfcr.jsp

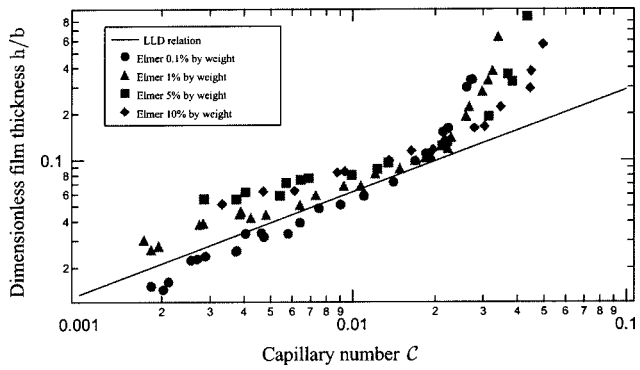

FIG. 14. Dimensionless film thickness versus capillary number for Elmer glue solutions.

$c/\mathrm{CMC}=25$, then monotonically decrease (e.g., Fig. 4 of Patist *et al.*[21]) and are reproduced in the overlay of Fig. 13. The ratio of $t_{\mathrm{micelle}}/t_{d2}$ thus reaches a maximum value of ~ 2. In this regime, when $t_{\mathrm{micelle}} \sim t_d$, the background concentration of monomer in the bulk will be depleted, this will limit the replenishment of surfactants to the interface and result in the reappearance of large surfactant surface concentration gradients. The resulting Marangoni stress will lead to a new increase in the thickening factor which should be of the same order as observed when $\phi \sim 1$. These arguments are consistent with the data at high concentrations shown in Fig. 12.

(iv) As the concentration increases beyond $\phi \approx 25$, the shape of the micelles becomes cylindrical, and there will be a concomitant decrease[33] in the micellar lifetime. Therefore, the limiting process returns once again to the bulk diffusion controlled case, so that the Marangoni stress increases and thickens the film.

For nonionic surfactants such as Triton X-100, less is known about the micellar lifetime for $\phi \gg 1$, although near the CMC the micellar lifetime appears to decrease.[33] The maximum micellar lifetime is measured to be ~ 3.5 s which is less than $t_{d2}=6.2$ s. Thus, monomer resupply mechanism will not be active and the thickening factor will not show a second maximum.

Many of the observations documented in this paper (as well as those given in the references) are characteristic of coating flows with more complicated complex fluids. To illustrate this point we report in Fig. 14 results of film thickness versus the capillary number for solutions made from solution of the commercial Elmer's glue (a polyvinyl alcohol latex). This glue is representative of many complex fluids, as it contains different surfactants and suspended particles/colloids (no information on the chemical composition is available from the product or the company's website). We mixed distilled water with Elmer's glue to obtain solutions of various concentrations and observed that the film thickness increases as the latex concentration increases. This behavior is expected since (i) Marangoni-enhanced film thickening occurs, measured surface tensions decrease by 10–20% over this concentration range and (ii) fluid viscosity increases as the latex concentration increases. Two other observations are worth noting. With the addition of surfactants, wetting of the fiber occurs for the lowest capillary numbers studied (e.g., also, compare with Fig. 4 and figures for each of the surfactant systems studied), in contrast to measurements with pure water. Furthermore, as fiber speed increases there is a critical value where the film abruptly thickens. As discussed in Sec. II, this is an inertial effect and the critical speed at which the film diverges is $U_{\mathrm{crit}} \approx \sqrt{\gamma/b\rho}$, hence $\mathcal{C}_{\mathrm{crit}} \propto \gamma^{-1/2}$. Adding surfactants shifts this inertial response since the surface tension is lower for the surfactant solutions than that of the pure system and the higher viscosities of the more concentrated solutions also increase the capillary number. This trend is clearly illustrated with the Elmer's glue data shown in Fig. 14.

Understanding the dynamic surface tension is important for understanding the dynamics of fiber coating with surfactants. When the fluid is in motion, the equilibrium surface tension value might never be reached, and the actual surface tension will be higher than the static surface tension value; this effect is important for all of the results in this paper. For high molecular weight surfactants the interfacial rheology may also become important and large deformation rates along the interface may result in appreciable surface viscoelastic effects. We are currently investigating such issues using protein surfactants such as BSA.

ACKNOWLEDGMENTS

We thank PPG Industries and the Harvard MRSEC for support of this research and gratefully acknowledge support from C. H. Smith, P. Westbrook, and J. Yu. We thank D. Quéré and J. Ashmore for many helpful conversations.

APPENDIX: THE THIN FILM EQUATIONS

We present a brief derivation of the LLD relation and show how limiting cases for the thickening factors, e.g., $\alpha = 2^{2/3}$ and $4^{2/3}$, depend on the velocity distribution along the fluid–air interface. Generally, the surface velocity is a complicated function of the surfactant concentration at the interface, which, as has been illustrated in the many experiments discussed in the text, further depends on the chemical kinetics of the specific surfactant species.

Assume that a fiber is pulled at speed U through a fluid reservoir containing either a pure Newtonian fluid or a surfactant solution (see Fig. 1). In the fluid bulk, we have the continuity and Navier–Stokes equations for steady-state conditions,

$$\nabla \cdot \mathbf{v} = 0 \quad \text{and} \quad \rho \mathbf{v} \cdot \nabla \mathbf{v} = -\nabla p + \mu \nabla^2 \mathbf{v}, \tag{A1}$$

where ρ is the density, p is the pressure, $\mathbf{v}=(u,v)$ is the fluid velocity, and μ is the shear viscosity. Along the interface $y = h(x)$ we impose the boundary conditions of zero normal velocity and the normal and tangential stress balances; the latter involves the Marangoni stress generated by the surface tension gradient. On the fiber, the no-slip boundary condition is imposed.

Where dynamical effects are important in the film formation process, the films are thin, $|h_x| \ll 1$, and the foregoing

Downloaded 03 Jan 2003 to 18.80.1.86. Redistribution subject to AIP license or copyright, see http://ojps.aip.org/phf/phfcr.jsp

problem is specialized to a two-dimensional setting by introducing coordinates x and y along and perpendicular to the fiber (see Fig. 1). At leading order, the bulk equations (A1) reduce to the standard lubrication equations:

$$u_x+v_y=0, \quad p_y=0, \quad \text{and} \quad \mu u_{yy}=p_x, \tag{A2}$$

where subscripts indicate partial derivatives. At $y=0$, we have $u=U$ and at $y=h(x)$,

$$p=-\gamma h_{xx} \quad \text{and} \quad \mu u_y=\gamma_x. \tag{A3}$$

For our purposes here, it is convenient to introduce the (unknown) surface velocity $u_s(x)$ at $y=h(x)$ and to not explicitly use the tangential stress boundary condition in (A3). In view of (A2), (A3), and the no-slip condition at the fiber surface, we find

$$u(x,y)=U+\frac{(u_s(x)-U)}{h}y-\frac{(\gamma h_{xx})_x}{2\mu}(y^2-hy). \tag{A4}$$

The corresponding flow rate q is constant and given by

$$q=\int_{y=0}^{h(x)}u(x,y)\,dy=\frac{1}{2}h(u_s(x)+U)+\frac{h^3}{12\mu}(\gamma h_{xx})_x. \tag{A5}$$

We are interested in determining the film thickness $h(x\to\infty)=h_\infty$. There are three special cases depending on the surface velocity $u_s(x)$.

(I) With a pure Newtonian fluid, the surface tension γ is a constant, hence the shear stress on the interface is zero, i.e., $u_y=0$ at $y=h(x)$, which implies that $(u_s-U/h)=(\gamma h/2\mu)\,h_{xxx}$. Furthermore, $q=Uh_\infty$, and consequently we obtain

$$U(h-h_\infty)+\frac{\gamma h^3}{3\mu}h_{xxx}=0. \tag{A6}$$

Next, we introduce dimensionless variables by choosing $H=h/h_\infty$ and $X=x/\ell_I$, where $\ell_I=h_\infty/(3\mathcal{C})^{1/3}$, with the capillary number defined by $\mathcal{C}=\mu U/\gamma$. We thus find

$$H^3H_{XXX}=(1-H), \tag{A7}$$

which describes the dimensionless film thickness $H(X)$. This profile must match with the curvature of the fiber as the film thickens, which yields the requirement $h_{xx}\approx 1/b$ as $x\to\infty$ or $H_{XX}(\infty)\approx(3\mathcal{C})^{-2/3}h_\infty/b$; i.e., $h_\infty/b=(3\mathcal{C})^{2/3}H_{XX}(\infty)$. After integrating the ordinary differential equation (A7), we find $H_{XX}(\infty)=0.643$, and so the film thickness $h_\infty/b=1.34\mathcal{C}^{2/3}$, which is the well-known LLD relation.

(II) Motivated by the possibility that surfactants may act to rigidify an interface, we apply the constraint that the surface velocity $u_s=0$, as considered by Bretherton.[6] The corresponding flow rate is now $q=\frac{1}{2}Uh_\infty$, which is only half of the traditional LLD flow rate, and hence, we find the film profile changes according to

$$U(h-h_\infty)+\frac{\gamma h^3}{6\mu}h_{xxx}=0. \tag{A8}$$

In this case we nondimensionalize using $\ell_{\mathrm{II}}=h_\infty/(6\mathcal{C})^{1/3}$ and $X=x/\ell_{\mathrm{II}}$, which yields the same differential equation (A7). The film thickness now has the form $h_\infty/b=(6\mathcal{C})^{2/3}H_{XX}(\infty)$ or a thickening factor [see Eq. (A7)] $\alpha=2^{2/3}$ larger than the original LLD value.

(III) Stretching of the interface by fiber coating produces an interfacial stress that tends to increase the surface velocity. The Marangoni stress γ_x can be expressed as

$$\gamma_x=-\frac{(\gamma h_{xx}h)_x}{2}+\frac{\mu}{h}(u_s(x)-U). \tag{A9}$$

Since $u_s\leqslant U$, the maximum Marangoni stress occurs when $u_s=U$, i.e., the film on the surface is moving at the same speed as the fiber. In this case, $q=Uh_\infty$ and

$$U(h-h_\infty)+\frac{\gamma h^3}{12\mu}h_{xxx}=0. \tag{A10}$$

We thus nondimensionalize with $\ell_{\mathrm{III}}=h_\infty/(12\mathcal{C})^{1/3}$ and $X=x/\ell_{\mathrm{III}}$, which again yields the differential equation (A7) and the final dimensional film thickness $h_\infty/b=(12\mathcal{C})^{2/3}H_{XX}(\infty)$. Thus, there is a film thickening factor $\alpha=4^{2/3}$, which shows that the maximum thickening factor is expected when the Marangoni stress is the strongest.

[1] S. F. Kistler and P. Schweizer, *Liquid Film Coating—Scientific Principles and Their Technological Implications* (Kluwer Academic, Dordrecht, 1997).
[2] D. Quéré, A. de Ryck, and O. ou Ramdane, "Liquid coating from a surfactant solution," Europhys. Lett. **37**, 305 (1997).
[3] D. Quéré, "Fluid coating on a fiber," Annu. Rev. Fluid Mech. **31**, 347 (1999).
[4] L. Landau and B. Levich, "Dragging of a liquid by a moving plate," Acta Physicochim. URSS **17**, 42 (1942).
[5] B. Derjaguin, "On the thickness of the liquid film adhering to the walls of a vessel after emptying," Acta Physicochim. URSS **20**, 349 (1943).
[6] F. P. Bretherton, "The motion of long bubbles in tubes," J. Fluid Mech. **10**, 166 (1961).
[7] J. A. Tallmadge and D. A. White, "Film properties and design procedures in cylinder withdrawal," I&EC Process Des. Dev. **7**, 503 (1968).
[8] D. Quéré and A. de Ryck, "Inertial coating of a fiber," J. Fluid Mech. **311**, 219 (1996).
[9] O. Ou Ramdane and D. Quéré, "Thickening factor in Marangoni coating," Langmuir **13**, 2911 (1997).
[10] A. de Ryck and D. Quéré, "Fluid coating from a polymer solution," Langmuir **14**, 1911 (1998).
[11] J. A. Tallmadge, "Withdrawal of flat plates from power law fluids," AIChE J. **16**, 925 (1970).
[12] D. Quéré and A. de Ryck, "Le mouillage dynamique des fibres," Ann. Phys. **23**, 1 (1998).
[13] X. Fanton and A. M. Cazabat, "Spreading and instabilities induced by a solutal Marangoni effect," Langmuir **14**, 2554 (1998).
[14] A. L. Bertozzi, A. Munch, X. Fanton, and A. M. Cazabat, "Contact line stability and undercompressive shocks in driven thin film flow," Phys. Rev. Lett. **81**, 5169 (1998).
[15] O. K. Matar and R. V. Craster, "Models for Marangoni drying," Phys. Fluids **13**, 1869 (2001).
[16] K. J. Stebe, S. Lin, and C. Maldarelli, "Remobilizing surfactant retarded fluid particle interfaces. I. Stress-free conditions at the interfaces of micellar solutions of surfactants with fast sorption kinetics," Phys. Fluids A **3**, 3 (1991).
[17] J. Ratulowski and H. C. Chang, "Marangoni effects of trace impurities on the motion of long gas bubbles in capillaries," J. Fluid Mech. **210**, 303 (1990).
[18] C. W. Park, "Effects of insoluble surfactants on dip coating," J. Colloid Interface Sci. **146**, 382 (1991).
[19] K. J. Stebe and C. Maldarelli, "Remobilizing surfactant retarded fluid particle interfaces. II. Controlling the surface mobility at interfaces of solutions containing surface active components," J. Colloid Interface Sci. **163**, 177 (1994).
[20] C. Ybert and J.-M. di Meglio, "Ascending air bubbles in solutions of

Downloaded 03 Jan 2003 to 18.80.1.86. Redistribution subject to AIP license or copyright, see http://ojps.aip.org/phf/phfcr.jsp

surface-active molecules: influence of desorption kinetics,'' Eur. Phys. J. E **3**, 143 (2000).
[21]A. Patist, S. G. Oh, R. Leung, and D. O. Shah, ''Kinetics of micellization: its significance to technological processes,'' Colloids Surf., A **176**, 3 (2001).
[22]P. D. T. Huibers, ''Surfactant self-assembly, kinetics and thermodynamics of micellar and microemulsion systems,'' Ph.D. thesis, University of Florida, 1996.
[23]A. de Ryck and D. Quéré, ''Entrainement visco-inertiel de liquide par un fil,'' C R. Acad. Sci. III **317**, 891 (1993).
[24]A. W. Adamson and A. P. Gast, *Physical Chemistry of Surfaces* (Wiley, Canada, 1997).
[25]B. J. Carroll and J. Lucassen, ''Capillarity-controlled entrainment of liquid by a thin cylindrical filament,'' Chem. Eng. Sci. **28**, 23 (1973).
[26]D. E. Graham and M. C. Phillips, ''Proteins at liquid interfaces,'' J. Colloid Interface Sci. **70**, 403 (1978).
[27]P. Sierro and D. Roux, ''Structure of a lyotropic lamellar phase under shear,'' Phys. Rev. Lett. **78**, 1496 (1997).
[28]S. L. Keller, P. Boltenhagen, D. J. Pine, and J. A. Zasadzinski, ''Direct observation of shear-induced structures in wormlike micellar solutions by freeze-fracture electron microscopy,'' Phys. Rev. Lett. **80**, 2725 (1998).
[29]C. H. Chang and E. I. Franses, ''Adsorption dynamics of surfactants at the air/water interface: a critical review of mathematical models, data, and mechanisms,'' Colloids Surf., A **100**, 1 (1995).
[30]R. Bel Fdhila and P. C. Duineveld, ''The effect of surfactant on the rise of a spherical bubble at high Reynolds and Peclet numbers,'' Phys. Fluids **8**, 310 (1996).
[31]R. Miller, V. B. Fainerman, A. V. Makievski, J. Kragel, D. O. Grigoriev, V. N. Kazakov, and O. V. Sinyachenko, ''Dynamics of protein and mixed protein/surfactant adsorption layers at the water/fluid interface,'' Adv. Colloid Interface Sci. **86**, 39 (2000).
[32]S. S. Datwani and K. J. Stebe, ''The dynamic adsorption of charged amphiphiles: The evolution of the surface concentration, surface potential, and surface tension,'' J. Colloid Interface Sci. **219**, 282 (1999).
[33]C.-U. Hermann and M. Kahlweit, ''Kinetics of micellization of Triton X-100 in aqueous solutions,'' J. Phys. Chem. **84**, 1536 (1980).

Downloaded 03 Jan 2003 to 18.80.1.86. Redistribution subject to AIP license or copyright, see http://ojps.aip.org/phf/phfcr.jsp